GEOPHYSICAL RESEARCH LETTERS, VOL. ???, XXXX, DOI:10.1029/,

The impact of midlatitude stationary waves on regional Hadley cells and ENSO

Rodrigo Caballero

Meteorology and Climate Centre, School of Mathematical Sciences,

University College Dublin, Ireland.

Bruce T. Anderson

Department of Geography and Environment, Boston University, Boston,

Mass., USA.

Rodrigo Caballero, Meteorology and Climate Centre, School of Mathematical Sciences, University College Dublin, Belfield, Dublin 4, Ireland. (rodrigo.caballero@ucd.ie)

Bruce T. Anderson, Department of Geography and Environment, Boston University, 675 Commonwealth Ave., Boston, MA 02215, USA, (brucea@bu.edu)

Stationary planetary waves are excited in the midlatitudes, propagate equatorward and are absorbed in the subtropics. The impact these waves have on the tropical climate has yet to be fully unraveled. Previous work has shown that interannual variability of zonal-mean stationary eddy stress is well correlated with interannual variability in Hadley cell strength. A separate line of research has shown that changes in midlatitude planetary waves local to the Pacific strongly affect ENSO variability. Here, we show that the two phenomena are in fact closely connected. Interannual variability of wave activity flux impinging on the subtropical central Pacific affects the local Hadley cell. The associated changes in subtropical subsidence affect the surface pressure field and wind stresses, which in turn affect ENSO. As a result, a winter with an anomalously weak Hadley cell tends to be followed a year later by an El Niño event.

1. Introduction

In the subtropical upper troposphere, the leading order zonal momentum balance is

$$(f + \overline{\zeta})\overline{v} \approx S, \tag{1}$$

a balance between the meridional transport of zonal-mean absolute vorticity by the Hadley cell, $(f+\overline{\zeta})\overline{v}$, and the eddy momentum flux convergence or Reynolds stress S, due mostly to extratropical eddies propagating equatorward. This balance suggests that extratropical eddies can play a major role in controlling the Hadley cell mass flux, as shown in a number of studies employing idealized atmospheric models [*Becker et al.*, 1997; *Becker and Schmitz*, 2001; *Kim and Lee*, 2001; *Walker and Schneider*, 2005, 2006; *Schneider*, 2006; *Schneider and Bordoni*, 2008; *Bordoni and Schneider*, 2008].

In previous work [*Caballero*, 2007], we sought observational corroboration of this idea and found that interannual variability in Northern Hemisphere winter Hadley cell mass flux is well correlated with eddy stress fluctuations, which in fact statistically explain a larger fraction of the Hadley cell variance than ENSO. We also found that *stationary* eddies have the dominant effect (see Sec. 2 below).

Here, we expand on this previous work, which dealt exclusively with the zonal-mean circulation, by applying a range of diagnostic tools to elucidate the geographical structure of the fluctuations. We show (Sec. 3) that stationary wave-Hadley cell interactions are focused in two zonally-confined regions, one in the central Pacific and the other in the east Atlantic/North Africa. In each of these sectors, anomalously strong wave stress drives a locally enhanced Hadley cell. Interestingly, it turns out that the local Hadley cell enhancement over the Pacific also affects the phase of ENSO (Sec. 4). This finding connects with and sheds new light on previous work on extratropical forcing of ENSO [*Vimont et al.*, 2003; *Anderson*, 2003].

2. Hadley cell strength and its variability

This section gives a more technical review of previous results, with the purpose of introducing key concepts and notation used in the rest of the paper. A standard measure of Hadley cell strength during December–February (DJF) is the index ψ^N introduced by *Oort and Yienger* [1996], defined as the maximum value of the seasonal-mean isobaric mass streamfunction between 0° and 30°N. In *Caballero* [2007], ψ^N was computed using the ERA40 reanalysis product [*Uppala et al.*, 2005]; the resulting time series was then detrended and partitioned into two components,

$$\psi^N = \psi_e^N + \psi_r^N, \tag{2}$$

where ψ_e^N is a linear regression onto the El Niño 3.4 index [*Trenberth*, 1997], while ψ_r^N is an uncorrelated remainder. It was then shown that fluctuations in ψ_r^N are associated with changes in stationary eddy stress

$$S_{st} = -\frac{1}{a\cos^2\varphi}\frac{\partial}{\partial\varphi}\left(\cos^2\varphi[\overline{u^*}\ \overline{v^*}]\right), \tag{3}$$

where seasonal and zonal averages are represented by an overbar and square brackets respectively, while asterisks indicate deviations from the zonal mean. Since ψ_r^N accounts for about 75% of the total ψ^N variance (after detrending), it was concluded that changes in stationary eddy stress exert a dominant control over interannual variability of DJF Hadley cell strength.

3. Wave activity diagnostics

The chief diagnostic tool we use here is the wave activity flux F_s introduced by *Plumb* [1985]. F_s is a vector approximately parallel to the local group velocity of stationary Rossby waves, tracking their propagation from regions of wave generation (where F_s diverges) to regions of dissipation (where F_s converges). The propagation of Rossby waves entails a momentum flux directed opposite to the wave motion. As a result, zones of mean wave dissipation (and thus of wave activity convergence) are also regions of zonal-mean deceleration. Mathematically, the zonally averaged horizontal convergence of F_s is equal to the stationary eddy stress S_{st}.

As in *Caballero* [2007], we employ the ERA40 reanalysis and focus on the boreal winter season (DJF) for the years 1958 to 2001. Figure 1 shows composites of upper-tropospheric F_s (computed as in Eq. (5.7) of *Plumb* [1985]) and its horizontal convergence. Climatologically, there are three main regions of wave activity convergence in the subtropics: one over the western Pacific, another stretching from the central Pacific to North America, and a third over the eastern Atlantic and northern Africa. The west Pacific convergence region is due to absorption of strong, southward-propagating wave activity emanating from the Asian continent. The fraction of wave activity not absorbed in the western Pacific is refracted into an eastward-flowing stream centered around 20°N, which then collides with northward-flowing, cross-equatorial wave activity flux forming the strong convergence region in the eastern Pacific. A second stream of wave activity emerges from the Asian mainland at higher latitudes, which arcs across the Pacific and North America and propagates southward in the Atlantic, where it is absorbed over western North Africa.

During high ψ_r^N years (Fig. 1a), the zonally-oriented wave activity stream in the subtropical Pacific is tilted equatorward, and there is wave absorption throughout the central and eastern basin. There is also strong southward wave activity flux in the Atlantic, and strong wave absorption in the subtropical Atlantic/North Africa. Conversely, in low ψ_r^N years the subtropical Pacific wave activity stream is oriented either directly eastward or even tilts *northward*, away from the subtropical absorption region. In the Atlantic, wave activity flux is still southward but is much weaker. The difference between high- and low-ψ_r^N years can be more clearly seen in Fig. 1c, showing regressions of ψ_r^N onto wave activity flux and its horizontal convergence. Strong, southward-oriented flux anomalies are apparent in both the Pacific and Atlantic basins, accompanied by convergence anomalies in the subtropical central Pacific and North Africa. Overall, low ψ_r^N years have much weaker zonally-integrated wave activity flux convergence in the subtropics and thus weaker S_{st}, in agreement with *Caballero* [2007].

One wonders if the Pacific and African eddy stress anomalies occurs synchronously or if they are independent. To address this question, we form a Pacific eddy stress index S_{st-Pac} by averaging the wave activity flux convergence for each season over a Pacific box (10°–20°N, 175°E–140°W), and an analogous Atlantic/North African index S_{st-Atl} using the box 15°–25°N, 0°–40°E. The resulting indices have a Pearson correlation coefficient of 0.51, which is significant at the 99.9% level assuming no autocorrelation.

Figure 2 shows a regression of ψ_r^N on seasonal-mean vertical velocity. In the zonal mean, there is enhanced sinking in the subtropics and ascent along the equator, as expected—ψ_r^N is, after all, an index of Hadley cell mass flux. However, the mass flux anomalies are far from zonally uniform. There is strong Hadley cell enhancement in the central to eastern Pacific, and more moderate enhancement over North Africa; these locations correspond closely with the regions of anomalous stationary eddy stress identified above.

The picture that emerges is one of Pacific and Atlantic stationary wave anomalies that are largely synchronous and coherently affect the Hadley cell. The Pacific-Atlantic linkage found here is reminiscent of recent work by *Strong and Magnusdottir* [2008], who find that Rossby wave breaking events in the Pacific lead to anomalous wave activity propagation across North America into the Atlantic, where they affect the phase of the North Atlantic Oscillation (NAO). This impression is further supported by a regression of ψ_r^N on seasonal-mean sea level pressure (SLP), Fig. 2, which shows a dipole signature in the North Atlantic very similar to the NAO pattern.

4. Relation to ENSO

There is a considerable body of work [*Barnett*, 1985; *Trenberth and Shea*, 1987; *Chan and Xu*, 2000; *Vimont et al.*, 2003; *Anderson*, 2003] documenting the impact of mid-latitude variability on the tropical Pacific basin. Specifically, winter-season midlatitude atmospheric circulation anomalies force subtropical SLP and surface windstress anomalies, which in turn affect equatorial ocean-atmosphere dynamics favoring the occurrence of ENSO events a year later, thereby overcoming the "spring predictability barrier" associated with the evolution of ENSO-related sea surface temperatures prior to and following boreal spring [*Webster and Yang*, 1992].

As noted by *Vimont et al.* [2003], the SLP variability in question has a spatial structure resembling the North Pacific Oscillation (NPO). *Linkin and Nigam* [2008] have recently emphasized the connection between the NPO and upper-level dipole anomalies, suggesting that the NPO is in fact a troposphere-filling equivalent-barotropic mode. Regression of ψ_r^N onto SLP (Fig. 2) shows a north-south dipole in the Pacific which also resembles the NPO, and regression onto the upper-level streamfunction (Fig. 1c) shows a coherent north-south dipole. The positive, equatorward lobe of the SLP dipole also corresponds closely with observed anomalies that precede ENSO events 12-15 months later [*Anderson*, 2003; *Vimont et al.*, 2003]. Its location to the north-east of Hawaii coincides with the subsiding branch of the locally-enhanced Hadley cell (Fig. 2).

To study the relationship between SLP anomalies in this region and ENSO, *Anderson* [2003] defined an SLP anomaly index (SLPI) as the seasonal-mean (November–March) SLP anomaly averaged over the region 150°-175°W and 10°-25°N, and showed that the SLPI is strongly anticorrelated with the January-March El Niño 3.4 index *Trenberth* [1997] during the winter of the *following* year ($r = -0.62$, significant at the 99% level). Here, we find that ψ_r^N is also anticorrelated with the El Niño 3.4 index a year later ($r = -0.53$) and is well correlated with SLPI ($r = 0.67$); both of these correlations are significant at the 99% level. As a result, a winter featuring anomalously strong stationary wave absorption in the central Pacific, and thus an anomalously strong local Hadley cell, will tend to be followed by a negative ENSO (i.e. La Niña) event a year later.

5. Summary and discussion

To summarize, we find that Hadley cell–stationary wave interaction is focused in two zonally-confined regions of the subtropics, one in the central Pacific and the other in the east Atlantic/North Africa. Anomalously strong wave stress drives locally-enhanced

Hadley circulations in these two regions. These regional fluctuations are often synchronous, suggesting they are teleconnected through inter-basin wave activity flux from the Pacific to the Atlantic. In the Pacific, the subsiding branch of the locally-enhanced cell is associated with a surface pressure anomaly whose impact on surface wind stress and heat fluxes can affect the phase of ENSO a year later.

Wave-mean flow interaction in the subtropical central Pacific plays the leading role in this narrative. It is therefore especially important to understand what controls the interannual changes in wave absorption observed there (Fig. 1). We emphasize again that the main difference between years with strong and weak Hadley circulation is that the former feature strong stationary wave absorption in the central Pacific, while during the latter much of the wave activity returns to the midlatitudes without absorption. One possibility is to take a linear WKB approach and suppose that interannual fluctuations in the Rossby wave refractive index create a central Pacific reflecting surface on some years which steers wave activity emanating from the Asian continent back into midlatitudes [see *Seager et al.*, 2003, for a similar argument applied to the zonal-mean flow].

To evaluated this hypothesis, we compute composites of the stationary wave number K_s [*Hoskins and Ambrizzi*, 1993] over years with positive and negative central Pacific eddy stress anomaly S_{st-Pac} (Fig. 3a and b respectively). K_s plays the role of Rossby refractive index: according to WKB theory, Rossby wave group velocities will be refracted away from low K_s toward high K_s [*Hoskins and Karoly*, 1981; *Hoskins and Ambrizzi*, 1993]. As Fig. 3 makes apparent, low K_s on the equatorward flank of the Pacific jet accounts for the eastward turning of the wave activity emanating from the Asian continent; the effect is stronger for shorter wavelengths, which propagate further toward the central Pacific. Comparing Figs. 3a and b shows very little difference in K_s, which results in very similar Rossby wave rays. The wave rays follow the wave activity flux vectors quite closely in the strong absorption case, Fig. 3a, suggesting that the dynamics is approximately linear in this case. On the contrary, the weak absorption case, Fig. 3b, shows large discrepancies between Rossby wave rays and wave activity flux in the central Pacific, implying that the northward turning of the wave activity flux in this case is not easily explained by simple linear dynamics.

An alternative possibility is that the differences in wave propagation are related to nonlinear reflection. Recent work has shown evidence for nonlinear reflection associated with Rossby wave breaking in both models and observations [*Walker and Magnusdottir*, 2003; *Abatzoglou and Magnusdottir*, 2004]. It is possible that different rates of wave breaking in different years could explain the changes in mean wave propagation seen in Fig. 3. Some support for this hypothesis is provided by the finding that reduced intra-seasonal, low-frequency variability over the central extratropical North Pacific (as represented by the variance in the daily SLP fields over 150–175°W, 20–45°N [see *Anderson*, 2007]) is well correlated with the seasonal-mean subtropical Pacific SLP signature of the intensified regional Hadley cell circulation seen in Fig 2.

Finally, we note that while we have chosen in this paper to focus on dynamical aspects, none of the results presented here excludes the possibility of diabatic heating in the tropics or subtropics playing a major role by either directly forcing Rossby waves that subsequently propagate poleward, or by modifying the subtropical flow and thus the absorption or reflection of extratropical waves at their critical latitudes. Mutually reinforcing interactions between dynamical processes and diabatic forcing, involving the coupled ocean-atmosphere system, are also conceivable. Disentangling this complex of interactions to arrive at the ultimate causes of the Hadley cell-stationary wave fluctuations documented here seems a worthwhile avenue for future work.

References

Abatzoglou, J. T., and G. Magnusdottir (2004), Nonlinear planetary wave reflection in the troposphere, *Geophys. Res. Lett.*, *31*, L9101, doi:10.1029/2004GL019495.

Anderson, B. (2003), Tropical Pacific sea-surface temperatures and preceding sea level pressure anomalies in the subtropical North Pacific, *J. Geophys. Res.*, *108*, 4732.

Anderson, B. (2007), Intraseasonal atmospheric variability in the extratropics and its relation to the onset of tropical Pacific sea surface temperature anomalies, *J. Climate*, *20*, 926–936.

Barnett, T. (1985), Variations in near-global sea level pressure, *J. Atmos. Sci.*, *42*, 478–501.

Becker, E., and G. Schmitz (2001), Interaction between extratropical stationary waves and the zonal mean circulation, *J. Atmos. Sci.*, *58*, 462–480.

Becker, E., G. Schmitz, and R. Geprägs (1997), The feedback of midlatitude waves onto the Hadley cell in a simple general circulation model, *Tellus Ser. A*, *49*, 182–199.

Bordoni, S., and T. Schneider (2008), Monsoons as eddy-mediated regime transitions of the tropical overturning circulation, *Nat. Geosci.*, *1*, 515–519.

Caballero, R. (2007), Role of eddies in the interannual variability of Hadley cell strength, *Geophys. Res. Lett.*, *34*, L22,705, doi:10.1029/2007GL030971.

Chan, J., and J. Xu (2000), Physical mechanisms responsible for the transition from a warm to a cold state of the El Niño–Southern Oscillation, *J. Climate*, *13*, 2056–2071.

Hoskins, B., and T. Ambrizzi (1993), Rossby wave propagation on a realistic longitudinally varying flow, *J. Atmos. Sci.*, *50*, 1661–1671.

Hoskins, B., and D. Karoly (1981), The steady linear response of a spherical atmosphere to thermal and orographic forcing, *J. Atmos. Sci.*, *38*, 1179–1196.

Kim, H.-K., and S. Lee (2001), Hadley cell dynamics in a primitive equation model. Part II: Nonaxisymmetric flow., *J. Atmos. Sci.*, *58*, 2859–2871.

Linkin, M., and S. Nigam (2008), The North Pacific Oscillation–West Pacific teleconnection pattern: Mature-phase structure and winter impacts, *J. Climate*, *21*, 1979–1997.

Oort, A. H., and J. J. Yienger (1996), Observed interannual variability in the Hadley circulation and its connection to ENSO, *J. Climate*, *9*, 2751–2767.

Plumb, R. (1985), On the three-dimensional propagation of stationary waves, *J. Atmos. Sci.*, *42*, 217–229.

Schneider, T. (2006), The general circulation of the atmosphere, *Ann. Rev. Earth Planet. Sci.*, *34*, 655–688.

Schneider, T., and S. Bordoni (2008), Eddy-mediated regime transitions in the seasonal cycle of a Hadley circulation and implications for monsoon dynamics, *J. Atmos. Sci.*, *65*, 915–934.

Seager, R., N. Harnik, Y. Kushnir, W. Robinson, and J. Miller (2003), Mechanisms of hemispherically symmetric climate variability, *J. Climate*, *16*, 2960–2978.

Strong, C., and G. Magnusdottir (2008), How Rossby wave breaking over the Pacific forces the North Atlantic Oscillation, *Geophys. Res. Lett.*, *35*, L10,706, doi: 10.1029/2008GL033578.

Trenberth, K., and D. Shea (1987), On the evolution of the Southern Oscillation, *Mon. Wea. Rev.*, *115*, 3078–3096.

Trenberth, K. E. (1997), The definition of El Niño, *Bull. Amer. Meteor. Soc.*, *78*, 2771–2777.

Uppala, S., et al. (2005), The ERA-40 re-analysis, *Quart. J. Roy. Meteor. Soc.*, *131*, 2961–3012.

Vimont, D., J. Wallace, and D. Battisti (2003), The seasonal footprinting mechanism in the Pacific: Implications for ENSO, *J. Climate*, *16*, 2668–2675.

Walker, C., and T. Schneider (2005), Response of idealized Hadley circulations to seasonally varying heating, *Geophys. Res. Lett.*, *32*, L06,813.

Walker, C. C., and G. Magnusdottir (2003), Nonlinear planetary wave reflection in an atmospheric GCM, *J. Atmos. Sci.*, *60*, 279–286.

Walker, C. C., and T. Schneider (2006), Eddy influences on Hadley circulations: Simulations with an idealized GCM, *J. Atmos. Sci.*, *63*, 3333–3350.

Webster, P. J., and S. Yang (1992), Monsoon and ENSO: Selectively interactive systems, *Quart. J. Roy. Meteor. Soc.*, *118*, 877–926.

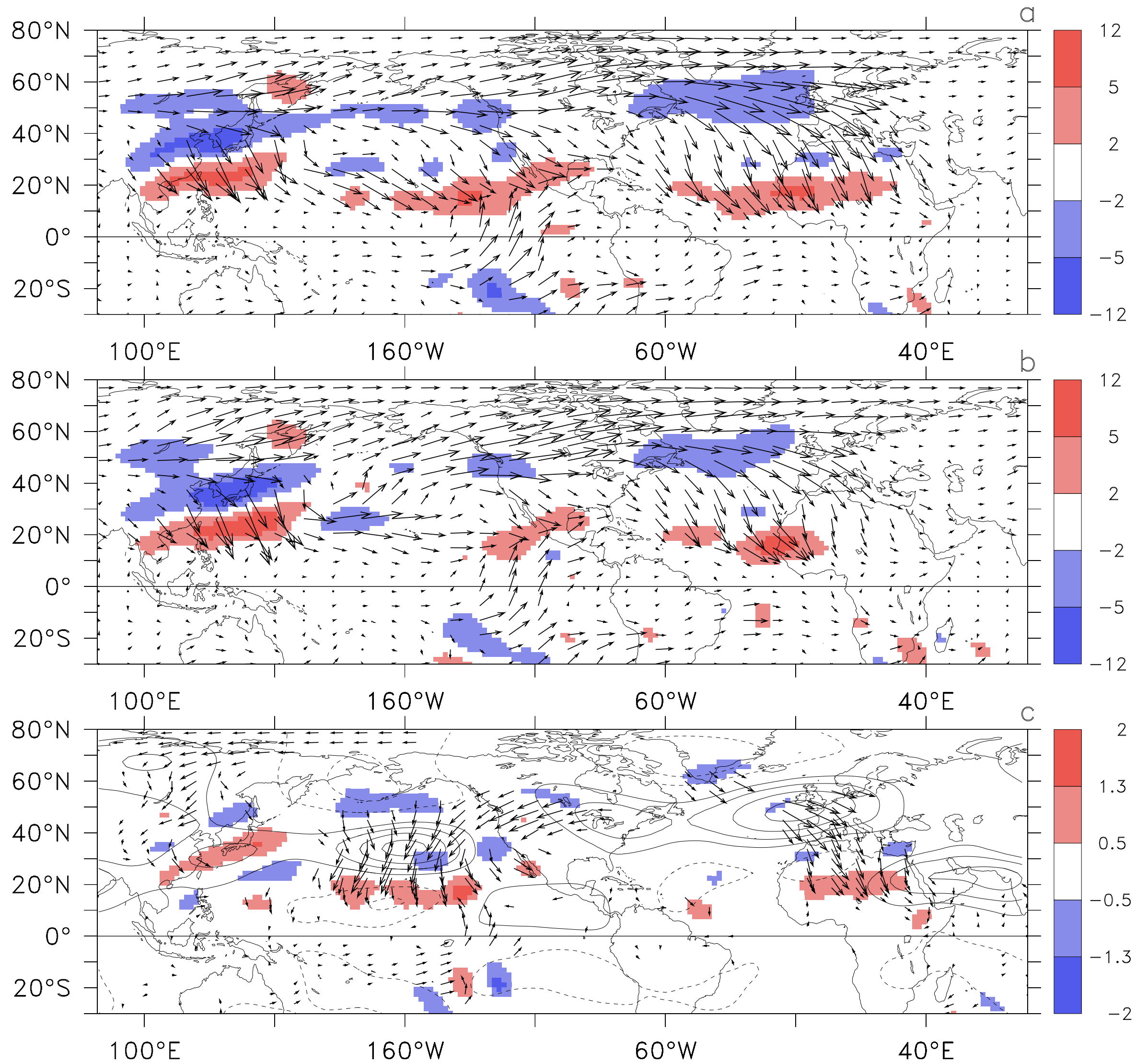

Figure 1. (a) Arrows show the DJF wave activity flux F_s at 250 hPa, with the longest arrow indicating about 100 m^2 s^{-2}. Shading shows the horizontal convergence of F_s, in units of m s^{-1} day^{-1}. Both quantities have been composited over years of anomalously high ψ_r^N (the 12 years with $\psi_r^N > \sigma/2$, where σ=1.4×10^{10} kg s^{-1} is the standard deviation of ψ_r^N). (b) As in (a) but composited over the 13 years with $\psi_r^N < -\sigma/2$. (c) Regression of ψ_r^N onto F_s (arrows, longest ∼ 25 m^2 s$^{-2}/\sigma$), the horizontal convergence of F_s (shading, units of m s^{-1} day$^{-1}/\sigma$), and the horizontal streamfunction (thin contours at intervals of 10^6 m^2 s$^{-1}/\sigma$). Wave activity regressions are shown only where they are statistically significant at the 95% level.

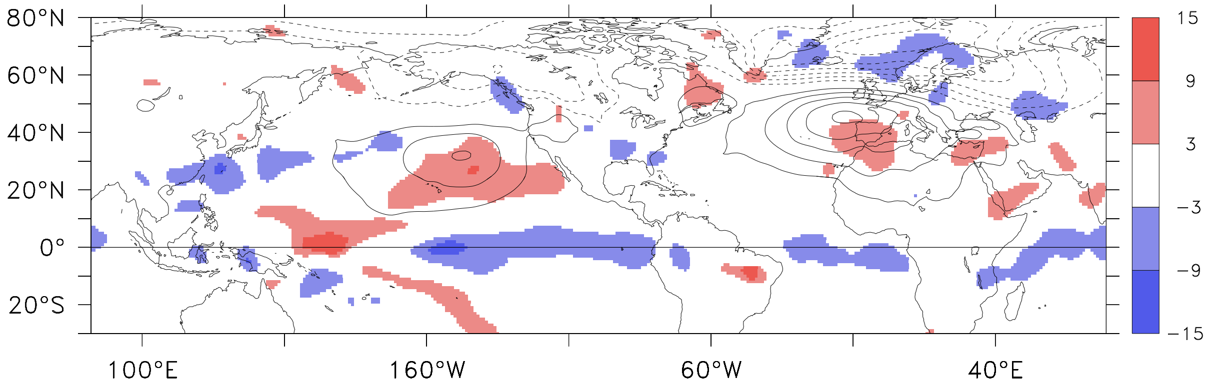

Figure 2. Regression of ψ_r^N onto DJF seasonal-mean pressure velocity, vertically averaged between 300 and 800 hPa and horizontally smoothed using an 11-point Parzen filter (shading, units of hPa day$^{-1}/\sigma$, where σ=1.4×10^{10} kg s^{-1} is the standard deviation of ψ_r^N) and sea level pressure (contours at 0.3 hPa/σ intervals, negative dashed and zero contour removed).

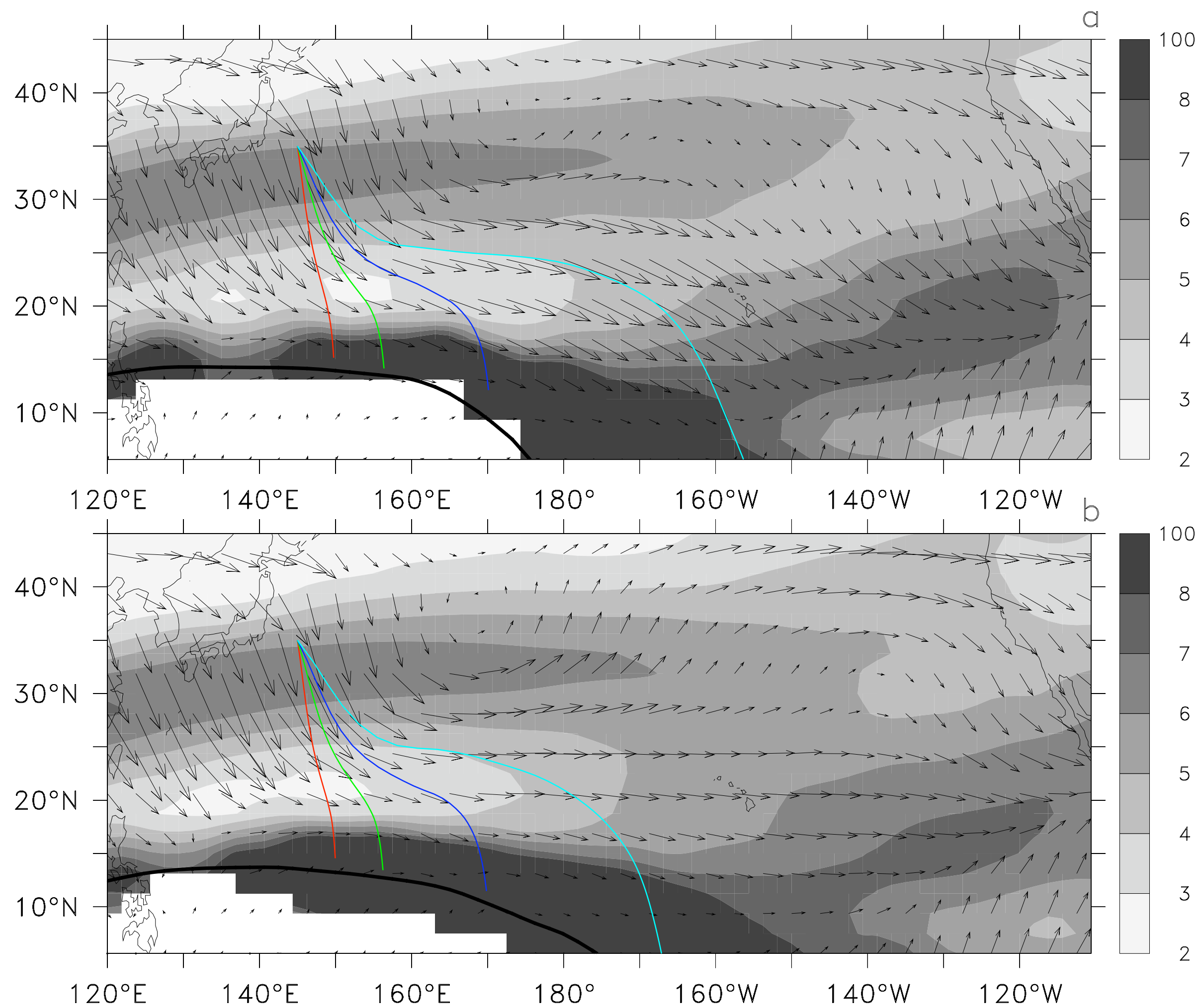

Figure 3. Pacific basin composites over (a) the 17 years with positive Pacific eddy stress anomaly S_{st-Pac}, and (b) the 26 years with negative anomaly (the asymmetry of these numbers reflects the skewness of the S_{st-Pac} frequency distribution). Arrows show the 250 hPa wave activity flux F_s as in Fig. 1. Shading shows the zonally-varying stationary wave number K_s at 250 hPa, computed as in Eq. (2.13) of *Hoskins and Ambrizzi* [1993] and smoothed with an 11-point Parzen filter. Coloured lines show ray tracing calculations starting at 40°N, 145°E, performed as in *Hoskins and Karoly* [1981] but using the full zonally-varying K_s, for zonal wavenumbers 1 (red), 2 (green), 3 (blue) and 4 (cyan). The thick black line shows the composite seasonal-mean zero wind line.